INTERNATIONAL JOURNAL OF AGRICULTURE & BIOLOGY
ISSN Print: 1560–8530; ISSN Online: 1814–9596
24–0033/2024/32–4–333–340
DOI: 10.17957/IJAB/15.2208
http://www.fspublishers.org

Full Length Article

Spatial Analysis of *Fimbristylis miliaceae* and Soil Properties for Site-Specific Weed Management in Harumanis Mango Cultivation

Nurul Aiza Mohd Fauzi, Khairun Nisa Kamarudin and Chuah Tse Seng*
Faculty of Plantation and Agrotechnology, Universiti Teknologi MARA, Perlis Branch, Arau Campus, 02600 Arau, Perlis, Malaysia
*For correspondence: chuahts@uitm.edu.my
Received 18 January 2024; Accepted 21 May 2024; Published 21 August 2024

Abstract

Understanding the spatial variation in soil properties and the distribution of weeds is essential for implementing sustainable weed management practices. This study aimed to investigate the spatial distribution of *Fimbristylis miliacea*, exploring the influence of soil properties on both their spatial distribution and density. Weed counts were conducted on a regular 20 × 20 m grid, comprising 60 observation points covering a study area of 2.49 hectares. The physico-chemical soil properties, including pH, temperature, moisture, organic total carbon, electrical conductivity (EC), total nitrogen (TN), available phosphorus, exchangeable potassium (Ex-K), exchangeable magnesium (Ex-Mg), exchangeable calcium (Ex-Ca) and exchangeable sodium (Ex-Na), were determined. The density of *F. miliaceae* exhibited a positive correlation with Ex-Na (r = 0.263) and Ex-Ca (r = 0.295). Geostatistical analysis revealed that the Gaussian model was best fitted to *F. miliaceae*, while the exponential model was suitable for both Ex-Ca and Ex-Na. The spatial distribution of these soil nutrients can be utilized to generate maps for targeted *F. miliaceae* management. These maps are crucial for making well-informed decisions regarding the site-specific management of *F. miliaceae* in Harumanis mango cultivation.

Keywords: *Fimbristylis miliaceae*; Geostatistical analysis; Physicochemical properties; Site-specific management; Spatial distribution

Introduction

Mango, scientifically known as *Mangifera indica* L., stands as a popular tropical fruit in South Asia, including Malaysia. Within the region, there exists a variety of mangoes, with 'Harumanis' emerging as the most favoured variety in the state of Perlis, Malaysia due to its distinctive aroma, texture, and sweetness. Over the years, the demand for Harumanis mango has steadily increased, resulting in a nearly tripled selling price per kilogram compared to other varieties. This trend has motivated local growers to expand their Harumanis mango cultivation, establishing it as a premium mango fruit prominently produced in Perlis (Azizan *et al.* 2019). The climatic conditions in Perlis play a crucial role in making the cultivation of the Harumanis mango feasible in the region. Specifically, the Harumanis mango tree requires a distinct dry period to initiate flowering. The flowering phase commences from January to February, with fruit-bearing occurring between March and April. Harvesting of the fruits takes place annually from May to June (Azizan *et al.* 2019).

In addition to climatic considerations, effective weed control stands as a top priority for farmers seeking to optimize economic returns. Farmers often engage in multiple concurrent weed management practices, encompassing the reduction of the weed seedbank, elimination of competitive weeds, prevention of new invasions, and combatting herbicide resistance (Somerville *et al.* 2020). Weeds pose a significant threat to crop yield, accounting for up to 34% of losses in agricultural and horticultural crop production (Somerville *et al.* 2020). The diverse density and scattered distribution of weed population presents challenges in devising effective weed management strategies (Partel *et al.* 2019; Somerville *et al.* 2019).

Fimbristylis miliacea (L.) Vahl, belonging to the Cyperaceae family, is sedge commonly found as a weed in rice fields. Its primary distribution encompasses tropical or subtropical regions in South and Southeast Asia, Central America, Northern Australia, and West Africa (Roy *et al.* 2019). *F. miliacea*, included in the Global Compendium of Weeds, is characterized as a tufted leafy annual or short-lived herb and is identified as both an agricultural and environmental weed (Randall 2012). In mango crop production, Olorunmaiye *et al.* (2013) reported considerable weed diversity, with 33 weed species identified. Similarly,

To cite this paper: Fauzi NAM, KN Kamarudin, CT Seng (2024). Spatial analysis of *Fimbristylis miliaceae* and soil properties for site-specific weed management in harumanis mango cultivation. *Intl J Agric Biol* 32:333–340

Rahim (2020) observed comparable weed diversity in both the mature mango canopy and inter-rows of both mature and immature mango trees, identifying 25, 22 and 24 weed species in mango, respectively. Among the prevalent weed species in mango, *F. miliaceae*, *Ageratum conyzoides* and *Mimosa pudica* L. were identified based on their highest relative abundance values.

Weed management in mango cultivation presents limited options. Farmers typically rely on manual weeding during the early stages of the crop or use small tools to control weeds within the plant rows. Mechanical weeding is another approach, utilizing bullock-drawn equipment or tractors equipped with specific attachments (Rana 2016). Intercropping with bitter gourd, chilies, or cowpea is also employed to suppress weed growth in mango orchards, interplanted (Rana 2016). However, chemical control, while effective against weeds, carries risks to human health and production. Commonly used herbicides such as glufosinate, diuron, bromacil, atrazine, and dalapon are effective against both grass and broadleaf weeds (Rana 2016).

Weed patches often remain in fixed locations over the years, as observed by various researchers (Gerhards and Christensen 2003; Kulkarni *et al.* 2017; Malmstrom *et al.* 2017). Numerous studies have highlighted associations between the patchy distribution of different weed species and the spatial heterogeneity of the soil. The presence of weeds is significantly influenced by soil organic carbon (SOC), soil texture, and nutrient status (Gaston *et al.* 2001; Nordmeyer and Häusler 2004; Korres *et al.* 2017). Kurniawati (2008) emphasized that weeds thrive in areas with good and fertile soil conditions that meet their living requirements.

Accurately assessing the spatial distribution of weeds is a crucial step for the effective implementation of weed management strategies at a given site. It is particularly pertinent for preventing the spread of weeds to clean areas, a concern that is highly relevant for new weed varieties, resistant strains, or emerging troublesome weeds. Employing site-specific weed management strategies based on mapping the patchy distribution of weeds can help control these unwanted plants (Castro *et al.* 2012).

Numerous studies have employed geostatistical analysis to investigate the spatial variability of soil nutrients in mango crop cultivation across various locations (Mali *et al.* 2016; Shahidin *et al.* 2018; Azizan *et al.* 2019). Metcalfe *et al.* (2015) noted that the relationship between weeds and environmental factors can differ depending on the scale, emphasizing the importance of incorporating scale-specific considerations in the development of models. The ideal mapping approach is contingent upon factors such as crop type, weed management systems, and considerations like data quality, quantity, and the intended application of the map (Somerville *et al.* 2020). In line with the findings of Patzold *et al.* (2020), maps were generated for management purposes to exemplify the correlation between weeds and soil. Nevertheless, there is insufficient information regarding the correlation between the distribution of *F. miliaceae* and soil properties. Hence, the objective of this study was to outline the spatial distribution of *F. miliaceae* and evaluate the impact of soil properties on their spatial distribution in mango. We studied *F. miliacea* due to its invasiveness and high abundance in Harumanis mango cultivation.

Materials and Methods

Experimental site

This study was carried out on a mature Harumanis mango plot (Plot B), one of the experimental plots at the Farm Unit of Universiti Teknologi MARA, Perlis Branch. Since 2010, 299 mango trees have been planted in a square planting technique with 9 m spacing between each tree on a total area of 2.49 hectares. The GPS coordinates are 6° 25' 46.9488" N and 100° 16' 11.4384" E, which correspond to Peninsular Malaysia's northern state at 53 m above sea level. Weed control in the research plot involved spraying herbicides, primarily using glufosinate ammonium, along with periodic mechanical slashing every two to three months.

Weed sampling and soil sampling

The weed survey was conducted in October 2022, one month after mechanical slashing during the vegetative stage of mango growth. The survey employed a systematic sampling method following a 20 × 20 m grid, resulting in 60 sampling units (Fig. 1). Traversal between points was conducted using a GPS receiver, specifically the Handheld Garmin GPS Map model (Edson and Wing 2012). This device was used to record and mark the coordinates of each sample point with varying degrees of accuracy. Each set of coordinates included latitude, longitude, and elevation data. Generally, latitude represented northing while longitude indicated easting. To facilitate mapping, these geographic coordinates were converted into a projected coordinate system. This transformation allowed for consistent measurements of lengths, angles, and areas on a flat, two-dimensional surface (Azizan *et al.* 2019). At each sample point, *F. miliaceae* plants were identified and counted within a fixed 1.0 square m area using a quadrat. Additionally, a total of 60 soil samples were collected systematically from grid sites using an auger, extracted from depths of 0 to 15 centims below the soil surface, also in October 2022.

Physicochemical properties of soil

Soil moisture and temperature were determined using a soil moisture and temperature probe concurrent with the soil sampling process. Subsequently, the gathered soil samples were allowed to naturally air-dry at room temperature for a period of seven days. Following this drying period, the samples underwent careful crushing using a porcelain pestle

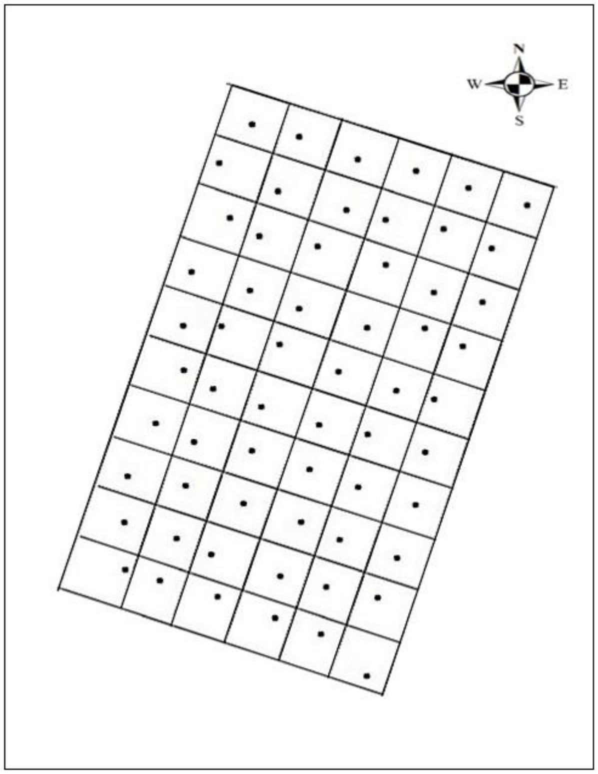

Fig. 1: A map indicating the sampling locations within a 2.49-hectare plot of mature Harumanis mango tree

and mortar. The crushed soil was then passed through a 2 mm mesh sieve for analysis of available phosphorus (Av-P), exchangeable potassium (Ex-K), calcium (Ex-Ca), sodium (Ex-Na) and magnesium (Ex-Mg). For the determination of total nitrogen (TN) and total carbon (TC), subsamples were meticulously sieved and ground to a particle size of Ø=250 μm. This finely ground soil was separated from any organic matter, charcoal, shells, rocks and plant seeds. The processed samples were subsequently employed to assess TC and TN content, utilizing an Elemental Analysis CHNSO Analyzer in accordance with the method outlined by Naik *et al.* (2010). Soil pH was determined by utilizing a pH m with a soil-to-water ratio of 1:2.5, while electrical conductivity (EC) was assessed using an EC m at a soil-to-water ratio of 1:5. In addition, the concentrations of available phosphorus (Av-P) were examined through spectrophotometry at 720 nm, employing the Bray II method described by Craze (1995). Moreover, Ex-K, Ex-Ca, Ex-Na and Ex-Mg in the soil samples were extracted using 1 M ammonium acetate buffered at pH 7. The concentrations of these elements were then analyzed using ICP-OES, following the procedure described by Lavkulich (1981).

Statistical analysis

The statistical analysis was conducted using IBM SPSS Statistics version 25 software. A normality test was executed to assess the normality of the data set ($P \leq 0.05$). For datasets exhibiting a non-normal distribution ($P \leq 0.05$), the Grubbs' Test (extreme studentized deviation test) was applied using GraphPad software to identify outliers. In order to prevent an increase in sample variance and skewed semivariograms, outliers were removed from the data set before performing geostatistical analysis, following the approach outlined by Oliver and Webster (2014). Given the non-normal distribution of all data sets, a Spearman correlation test was employed at a 5% significance level to determine the relationship between *F. miliaceae* density and soil properties. Weed density and soil nutrient data were analyzed with descriptive statistics, which included computing the mean, minimum, maximum, standard deviation and coefficient of variation.

Geostatistical analysis

The semivariogram models were employed to map the densities of *F. miliaceae*, Ex-Ca, and Ex-Na of the soil. The ArcGIS histogram tool was applied to scrutinize all data sets, considering their non-normal distribution. As per Environmental Systems Research Institute (ESRI) (2021c) guidelines, data were considered approximately normally distributed if the mean and median were similar, skewness was close to zero, and kurtosis was close to three (indicating a bell-shaped curve). Given the non-normal distribution of all data sets, log transformation was applied to stabilize their variance and approximate a normal distribution.

To evaluate the spatial variability of soil properties and weed density, a widely used and fundamental geostatistical semivariogram function was employed, as expressed in the following equation by Oliver and Webster (2014):

$$\hat{y}(\mathbf{h}) = \frac{1}{2m(\mathbf{h})} \sum_{i=1}^{m(\mathbf{h})} [z(\mathbf{x}_i) - z(\mathbf{x}_i + \mathbf{h})]^2$$

Where y(h) = empirical semivariogram; z (x_i) and z (x_i+h) = the observed values of z at places x_i and x_i+h; and m(h) = number of pairs of experimental points separated by a distance h.

The empirical semivariogram model was selected from a set of functions, including stable, circular, spherical, exponential, and Gaussian, as outlined by Obroślak and Dorozhynskyy (2017). Params for the nugget (C0), baseline (C0 + C), and range (A) effects were determined based on the model that best depicted the relationship between experimental semivariance and the h distance. To validate the accuracy of model estimator, cross-validation analysis was performed. This analysis included the examination of prediction errors such as mean error (ME), root-mean-square error (RMSE), average standard error (ASE), and root-mean-square standardized error (RMSSE). The equation for calculating prediction errors is provided below (Environmental Systems Research Institute (ESRI 2021b):

I. Mean error

$$\frac{\sum_{i=1}^{n}\left(\hat{Z}(s_i) - z(s_i)\right)}{n}$$

II. Root-mean-square error

$$\sqrt{\frac{\sum_{i=1}^{n}\left(\hat{Z}(s_i)-z(s_i)\right)^2}{n}}$$

III. Average error

$$\sqrt{\frac{\sum_{i=1}^{n}\hat{\sigma}(s_i)}{n}}$$

IV. Root-mean-square standardized error

$$\sqrt{\frac{\sum_{i=1}^{n}\left[\left(\hat{Z}(s_i) - z(s_i)\right)/\hat{\sigma}(s_i)\right]^2}{n}}$$

Let Zˆ (s_i) be the predicted value from cross-validation, let z (s_i) be the observed value, and let σˆ(s_i) be the prediction standard error for location (s_i).

The best fitted model selection criteria for soil each soil nutrient considered the mean error (ME) closest to zero, indicating an unbiased interpolation approach, the smallest root-mean-square error (RMSE), the average standard error (ASE) closest to the RMSE, and the root-mean-square standardized error (RMSSE) closest to one, as advocated by Panday *et al.* (2018) and Environmental Systems Research Institute (ESRI 2021a). To evaluate the spatial dependence index, the nugget to sill ratio (%) was calculated and classified as high (< 25%), moderate (25–75%), and weak (> 75%) spatial dependence, following the classification by Cambardella *et al.* (1994).

Following cross-validation, the selected semivariogram models were utilized to generate prediction maps for weed and soil properties. Ordinary kriging was employed for map interpolation to obtain the best linear unbiased predictions. The construction of semivariogram model params and prediction maps was performed using ArcGIS software ArcMap version 10.8. The geostatistical analysis was executed using the Geographic Information System (GIS) program ArcGIS version 10.8, in accordance with the approach outlined by Jurado-Exposito *et al.* (2021).

Results

Table 1 displays the descriptive statistics for *F. miliacea*, Ex-Ca, and Ex-Na of soil in the mango plot at UiTM Perlis. The calculated coefficient of variation (CV) values indicates varying degrees of variability in the experimental area. Specifically, *F. miliacea* exhibited a CV of 99.3%, Ex-Ca had a CV of 60%, and Ex-Na showed a CV of 30%.

Table 2 presents the adjusted semivariogram params for *F. miliaceae* density and soil characteristics, specifically

Table 1: Descriptive statistics on density of *F. miliaceae* and exchangeable calcium and sodium (*n = 60*)

	Mean	Minimun	Maximun	Standard deviation	Coefficient of variation (%)
F. miliaceae (no./m^2)	6	0	24	5.94	99.3
Calcium (cmol/kg)	0.10	0.04	0.33	0.06	60.0
Sodium (cmol/kg)	0.002	0.0008	0.003	0.0006	30.0

exchangeable calcium and exchangeable sodium to the theoretical model to determine the spatial variability in the experimental plot. The selection of the best adjustment model was determined through cross-validation, a critical analysis in choosing the theoretical semivariance model that most accurately reflects the empirical semivariance of the data. The results indicate that the mean error (ME) ranged from -0.0001 to 0.0000, root-mean-square error (RMSE) ranged from 0.0060 to 6.3625, average standard error (ASE) ranged from 0.0006 to 6.1325 and root-mean-square standardized error (RMSSE) ranged from 0.989 to 1.0392. These findings suggest acceptable accuracies in predicting weed density and each soil property from the generated maps. The range value for *F. miliaceae* was determined to be 300.08 m. The highest range for soil properties was 111.4 m for Ex-Ca, followed by Ex-Na with a range of 88.91 m. In this study, the most suitable models are the Gaussian and exponential models. The Gaussian model was applied to *F. miliaceae*, while the exponential model was employed for both soil properties (Ex-Ca and Ex-Na). The spatial dependence analysis categorized *F. miliaceae* and exchangeable calcium as having weak spatial dependence, whereas exchangeable sodium exhibited moderate spatial dependence.

Fig. 2 illustrates the distribution map of *F. miliacea* in the mature mango plot. Different shades of green on the map represent varying density levels of *F. miliacea* at different sampling sites. The darkest color corresponds to the highest density, while the brightest color indicates the lowest density. *F. miliacea* infestations were identified in the study area, with range values of 0–10 plants/m², showing a higher prevalence in the northeast region.

In Fig. 3a, the spatial variability map of Ex-Ca in the study area ranged from 0.06 to 0.14 cmol/kg indicating consistently low levels of Ex-Ca across almost all areas of the plot. Similarly, Fig. 3b illustrates the range of soil Ex-Na, which varied from 0.0011 to 0.002 cmol/kg across all areas of the plot, exhibiting very low levels. The northeast region in both Fig. 2, 3 displays the dark color, consistent with the correlation observed between *F. miliaceae* and Ex-Ca and Ex-Na in Table 3.

Discussion

The classification for coefficient of variation (CV) values

Table 2: Model parameters of the theoretical semivariograms and cross validation statistics for *F. miliaceae* and exchangeable calcium and sodium

	Model	Semivariogram parameters						Cross-validation			
		(C_0)[1/]	(C_0+C)[2/]	$\left(\frac{C_0}{C_0+C}\right)$[3/]	Range (m)	SDI[4/] (%)	*Spatial class	ME[5/]	RMSE[6/]	ASE[7/]	RMSSE[8/]
F. miliaceae	Gaussian	35.237	35.237	1.0	300.08	100	W	-0.1152	6.3625	6.1325	1.0374
Calcium	Exponential	0.0036	0.0044	0.8182	111.14	82	W	-0.0001	0.0626	0.0602	1.0392
Sodium	Exponential	2.5760	4.1134	0.6262	88.91	63	M	0.0000	0.0060	0.0006	0.989

*[1/]Nugget, [2/]Sill, [3/]Nugget/sill ratio, [4/]Spatial dependency index, [5/]Mean error, [6/]Root-mean-square error, [7/]Average standard error [8/]Root-mean-square standardized error.; M: moderate spatial dependency; W: weak spatial dependency

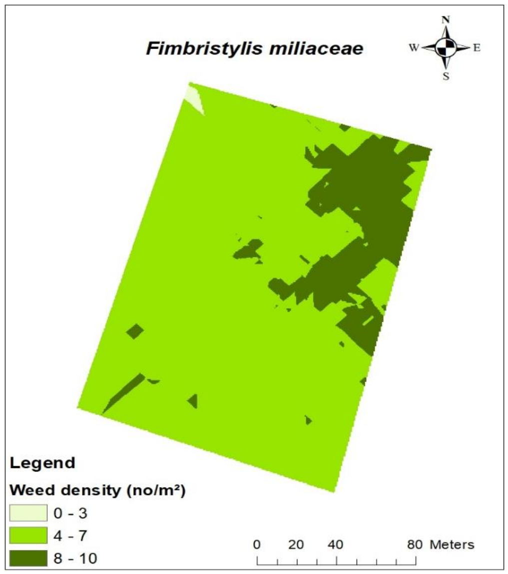

Fig. 2: Distribution map of *F. miliaceae*

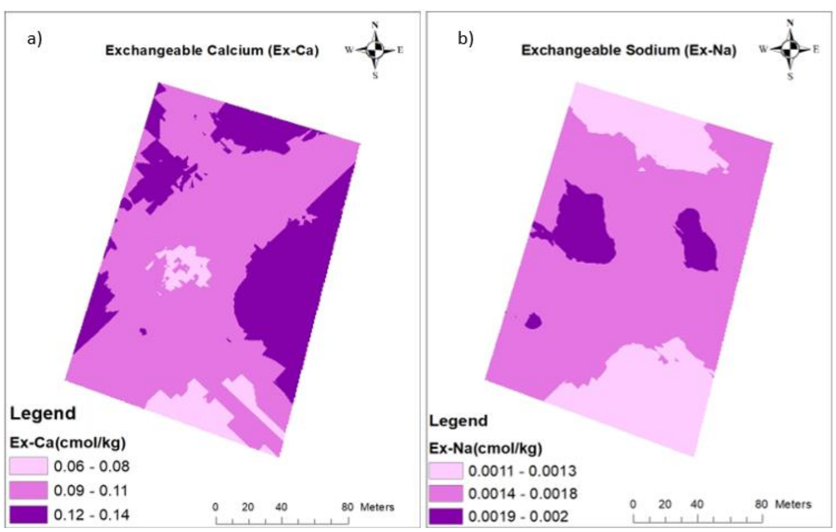

Fig. 3: Distribution maps of exchangeable calcium (**a**) and exchangeable sodium (**b**)

suggested by Vasu *et al.* (2017) indicates that CV < 15% is considered low, 15% ≤ CV ≥ 35% is moderate, and CV > 35% is high for soil nutrient variability. Furthermore, the coefficient of variation classification proposed by Warrick (1980) for weed density considers CV < 12% as low, 12% ≤ CV ≥ 60% as a and CV > 60% as high. The experimental area exhibited high variability in *F. miliaceae*, as indicated by a calculated coefficient of variation (CV) exceeding 60%. Similarly, Ex-Ca also demonstrated high variability, with coefficient of variation values surpassing 35%, in

Table 3: Correlation coefficients of *F. miliaceae* densities in relation to soil properties

Parameter	Correlation coefficient
Total nitrogen	0.679
Available phosphorus	-0.170
Exchangeable potassium	-0.008
Exchangeable calcium	0.295*
Exchangeable magnesium	0.165
Exchangeable sodium	0.263*
Total carbon	0.103
Soil temperature	0.014
Soil Moisture	-0.049
Electrical conductivity	-0.082
pH	0.199

*Significant correlation was noted at $P \leq 0.05$

contrast to Ex-Na, which showed moderate variability with a coefficient of variation value above 15% ≤ CV ≥ 35%.

The correlation coefficients between *F. miliaceae* densities and soil properties in Table 3 are comparable to the findings of Yousaf *et al.* (2022), who identified positive correlations between *Centella asiatica* (L.) Urb., *Malva parviflora* L. and *Cannabis sativa* L. with calcium. Additionally, Gibbons *et al.* (2017) reported positive correlations between leafy spurge and spotted knapweed cover with calcium. By contrast, Shiratsuchi *et al.* (2005) observed a negative correlation between *Cyperus rotundus* L., *Brachiaria plantaginea* (Link) R.D. Webster, and *Commelina benghalensis* L. with calcium. Gibbons *et al.* (2017) also found that cheatgrass had a negative correlation with calcium. According to Gibbons *et al.* (2017) noted that spotted knapweed cover has a negative correlation with sodium, which contradicts the present study's result indicating a positive correlation between *F. miliaceae* and sodium.

In addition, the outcomes obtained for model params of the theoretical semivariograms and cross-validation statistics concerning *F. miliaceae*, exchangeable calcium, and sodium align with Mali *et al.*'s (2016) observations (Table 2). Higher range values for specific soil params imply spatial dependency over extended distances, while lower range values indicate influences from neighboring values at shorter distances, distinguishing them from other variables. The Gaussian function employs a normal probability distribution curve, proving effective when phenomena exhibit similarity at short distances due to its gradual rise in semivariance (GISGeography 2022). Extrinsic factors such as agronomic practices are associated with weak spatial dependency, strong spatial dependency is linked to intrinsic factors like soil characteristics and mineralogy, and moderate spatial dependency results from a combination of internal and external variables (Cambardella *et al.* 1994; Mali *et al.* 2016).

On the other hand, site-specific management strategies for *F. miliacea* can be developed based on the weed maps generated in Fig. 2. According to Krahmer *et al.* (2020), weeds are often unevenly distributed within crops, suggesting that chemical or physical weed control measures should be applied only when necessary. Weed maps play a crucial role in crop-weed discriminating algorithms and decision support models assessing the weed risk in fields (Kavhiza *et al.* 2020). Integrating prescription maps with herbicide application technologies, such as patch spraying or variable rate treatment holds significant potential for effective weed control. This approach enables informed decision-making in agricultural fields by combining advanced sensor technologies with geographical information systems (GIS) (Zargar *et al.* 2018). Patch spraying, for instance, can be implemented using either weed maps or real-time sensors, with weed detection and spraying occurring simultaneously during real-time operations, unlike the separate activities involved in map-based spraying (Castaldi *et al.* 2017).

Fig. 3 presents spatial variability maps of calcium and magnesium levels within the mango plot, demonstrating correlations with the distribution of *F. miliaceae*. The study focuses on mango trees grown in lateritic soils, characterized as highly weathered tropical red soils with inherent low fertility, commonly classified as Ultisols in the U.S. Soil Taxonomy. The lack of information on nutrient composition in lateritic soil, considered problematic, could result in nutrient deficits if not managed appropriately (Nasron *et al.* 2021). Laterite soils typically exhibit moderate acidity in soil reaction and are associated with acidic parent materials and leaching of bases such as calcium, magnesium, potassium, and sodium from the soil (Nayak *et al.* 2002). Calcium tends to be less available in acidic soils and more available in alkaline soils (Bhindhu and Sureshkumar 2021). The deep hue observed in the northeast section of the test field (Fig. 2 and 3) corresponds with the relationships found between *F. miliaceae* density and soil calcium or sodium levels. This consistent spatial pattern underscores the impact of soil nutrient characteristics on the distribution of *F. miliaceae*. In other words, the spatial distribution of these soil nutrients can be utilized to generate maps for targeted *F. miliaceae* management. Given *F. miliaceae*'s affinity for calcium and magnesium-rich soil, farm-specific fertilization practices should be considered for tailored nutrient management, while ensuring the nutrient needs of Harumanis mango are not compromised.

Conclusion

In summary, the spatial distribution of *F. miliacea* was influenced by soil nutrient levels of calcium and sodium. Utilizing combined data on *F. miliacea* density and soil exchangeable sodium and calcium can aid in creating maps for targeted weed management. These maps are crucial for applying localized mechanical and chemical control strategies, ultimately improving the efficiency and cost-effectiveness of managing *F. miliacea*. Nonetheless, additional research is needed to investigate the relationship between *F. miliacea* density and soil calcium or sodium levels over multiple consecutive years for more accurate spatial distribution data.

Acknowledgements

The author expresses gratitude to the Faculty of Plantation and Agrotechnology (FPA) at University Technology MARA (UiTM) Perlis for granting permission to carry out the research project in the mango orchard. Special thanks are extended for the provision of facilities and laboratory materials essential for the study. The authors would like to thank Universiti Teknologi MARA, Shah Alam, Malaysia, for the research financial support (GIP: 600-RMC/GIP 5/3 (165/2021).

Author Contributions

Nurul Aiza Mohd Fauzi conducted the experimental work and drafted the manuscript, under the guidance of Chuah Tse Seng and Khairunnisa Kamarudin. Chuah Tse Seng provided assistance in interpreting the results and preparing the manuscript.

Conflicts of Interest

All authors declare no conflict of interest.

Data Availability

Data presented in this study will be available on a fair request to the corresponding author.

Ethics Approval

No approval is needed

References

Azizan FA, N Roslan, R Ruslan, AA Aznan, AZM Yusoff (2019). Soil NPK variability mapping for Harumanis mango grown in greenhouse at Perlis, Malaysia. *Intl J Adv Sci Eng Inform Technol* 9:495–501

Bhindhu PS, P Sureshkumar (2021). Availability indices of calcium and magnesium in soils of kerala. *J Trop Agric* 59:38–44

Cambardella CA, TB Moorman, JM Novak, TB Parkin, DL Karlen, RF Turco, AE Konopka (1994). Field-scale variability of soil properties in central Iowa soils. *Soil Sci Soc Amer J* 58:1501–1511

Castaldi F, F Pelosi, S Pascucci, R Casa (2017). Assessing the potential of images from unmanned aerial vehicles (UAV) to support herbicide patch spraying in maize. *Precis Agric* 18:76–94

Castro AID, M Jurado-Expósito, JM Peña-Barragán, F López-Granados (2012). Airborne multi-spectral imagery for mapping cruciferous weeds in cereal and legume crops. *Precis Agric* 13:302–321

Craze B (1995). *Soil Survey Standard Test Method: Available Phosphorus: Bray No 2 extract*. Department of Sustainable Natural Resources, New South Wales, Australia

Edson C, Wing M (2012). Tree Location Measurement Accuracy with a Mapping-Grade GPS. *For Sci* 58:567–576

Environmental Systems Research Institute (ESRI) (2021a). *Comparing models*. ArcGIS ArcMap 10.8. Redlands, CA. Available at https://desktop.arcgis.com/en/arcmap/latest/extensions/geostatistical-analyst/comparing-models.htm

Environmental Systems Research Institute (ESRI) (2021b). *Cross validation ArcGIS ArcMap 10.8*. Redlands, CA. Available at https://desktop.arcgis.com/en/arcmap/latest/tools/geostatistical-analyst-toolbox/cross-validation.htm

Environmental Systems Research Institute (ESRI) (2021c). *Histograms*. ArcGIS ArcMap 10.8. Redlands, CA. Available at https://desktop.arcgis.com/en/arcmap/latest/extensions/geostatistical-analyst/histograms.htm

Gaston LA, MA Locke, RM Zablotowicz, KN Reddy (2001). Spatial variability of soil properties and weed populations in the Mississippi Delta. *Soil Sci Soc Amer J* 65:449–459

Gerhards R, S Christensen (2003). Real-time weed detection, decision making and patch spraying in maize, sugarbeet, winter wheat and winter barley. *Weed Res* 43:385–392

Gibbons SM, Y Lekberg, DL Mummey, N Sangwan, PW Ramsey, JA Gilbert (2017). Invasive plants rapidly reshape soil properties in a grassland ecosystem. *MSystems* 2:e00178-16

GISGeography (2022). Semi-Variogram: Nugget, Range and Sill. Available at https://gisgeography.com/semi-variogram-nugget-range-sill/#3-exponential-models. (Accessed: 21 June 2022)

Jurado-Exposito M, F Lopez-Granados, FM Jimenez-Brenes, J Torres-Sanchez (2021). Monitoring the spatial variability of knapweed (*Centaurea diluta* Aiton) in Wheat Crops using geostatistics and UAV imagery: Probability maps for risk assessment in site-specific control. *Agronomy* 11:880

Kavhiza N (2020). Weed mapping technologies in discerning and managing weed infestation levels of farming systems. *Res Crops* 21:93–98

Korres NE, JK Norsworthy, KR Brye, VJR Skinner, A Mauromoustakos (2017). Relationships between soil properties and the occurrence of the most agronomically important weed species in the field margins of eastern Arkansas—Implications for weed management in field margins. *Weed Res* 57:159–171

Krahmer H, C Andreasen, G Economou-Antonaka, J Holec, D Kalivas, M Kolarova (2020). Weed surveys and weed mapping in Europe: State of the art and future tasks. *Crop Prot* 129:105010

Kulkarni SS, LM Dosdall, JR Spence, CJ Willenborg (2017). Field density and distribution of weeds are associated with spatial dynamics of omnivorous ground beetles (Coleoptera: Carabidae). *Agric Ecosyst Environ* 236:134–141

Kurniawati E (2008). *Perbedaan komposisi komunitas gulma pada area perkebunan teh rakyat dengan kanopi terbuka dan kanopitertutup di daerah pagilaran batang*. IKIP PGRI Semarang, Indonesia

Lavkulich LM (1981). *Methods Manual, Pedology Laboratory*. Department of Soil Science, University of British Columbia, Vancouver, British Columbia, Canada

Mali SS, SK Naik, BP Bhatt (2016). Spatial variability in soil properties of mango orchards in eastern plateau and hill region of India. *Vegetos* 29:74–79

Malmstrom CM, HS Butterfield, L Planck, CW Long, VT Eviner (2017). Novel fine-scale aerial mapping approach quantifies grassland weed cover dynamics and response to management. *PLoS One* 12:e0181665

Metcalfe H, AE Milne, R Webster, RM Lark, AJ Murdoch, J Storkey (2015). Designing a sampling scheme to reveal correlations between weeds and soil properties at multiple spatial scales. *Weed Res* 56:1–13

Naik S, VV Goud, PK Rout, K Jacobson, AK Dalai (2010). Characterization of Canadian biomass for alternative renewable biofuel. *Renew Ener* 35:1624–1631

Nasron N, NS Ghazali, NM Shahidin, AA Mohamad, SA Pugi, NM Razi (2021). Soil suitability assessment for Harumanis mango cultivation in UiTM Arau, Perlis. *IOP Conf Ser: Earth Environ Sci* 620:012007

Naya RK, GC Sahu, SSK Nanda (2002). Characterization and classification of soils of Central Research Station, Bhubaneswar. *Agropedology* 12:1–8

Nordmeyer H, A Häusler (2004). Einfluss von Bodeneigenschaften auf die Segetalflora von Ackerflächen (Impact of soil properties on weed distribution within agricultural fields). *J Plant Nutr Soil Sci* 167:328–336

Obroślak R, O Dorozhynskyy (2017). Selection of a semivariogram model in the study of spatial distribution of soil moisture. *J Water Land Dev* 35:161–166

Oliver MA, R Webster (2014). A tutorial guide to geostatistics: Computing and modelling variograms and kriging. *Catena* 113:56–69

Olorunmaiye P, S Taiwo,OO Alamu, K Egberongbe, PA Adeoye (2013). Assessment of weed species composition and species diversity in some fruit orchards.*Alban J Agric Sci* 12:215

Panday D, B Maharjan, D Chalise, R Kumar Shrestha, B Twanabasu (2018). Digital soil mapping in the Bara district of Nepal using kriging tool in ArcGIS. *PLoS One* 13:e0206350

Partel V, SC Kakarla, Y Ampatzidis (2019). Development and evaluation of a low-cost and smart technology for precision weed management utilizing artificial intelligence. *Comp Electr Agric* 157:339–350

Patzold S, C Hbirkou, D Dicke, R Gerhads, G Welp (2020). Linking weed patterns with soil properties: A long-term case study. *Precis Agric* 21:569–588

Rahim NH (2020). Characterizing weed population at two growth stages of Harumanis mango in Farm Unit Arau, Perlis. *Unpublished Bachelor's Thesis*. University Technology Mara Perlis

Rajender S, Rana (2016). *Weed Management of Orchards*. Department of Agronomy. CSK Himachal Pradesh, Palampur, India

Randall RP (2012). *A Global Compendium of Weeds*, p:124. Department of Agriculture and Food Western Australia. Perth, Australia. Available at: http://www.cabi.org/isc/FullTextPDF/2013/20133109119.pdf

Roy R, D Ud, AFM Shahid, A Akter, S Sultana, MA Barek, IJ Liya, MA Basher (2019). Antipyretic and anti-nociceptive effects of methanol extract of leaves of *Fimbristylis miliacea* in mice model. *J Ethnopharmacol* 243:112080

Shahidin NM, R Ismail, KN Kamarudin, SS Abe (2018). Spatial variability of selected chemical properties of a lateritic soil under mango cultivation in Northern Peninsular Malaysia. *Trop Agric Dev* 62:104–108

Shiratsuchi LSI, JRA Fontes, AV Resende (2005). Correlação da distribuição espacial do banco de sementes de plantas daninhas com a fertilidade dos solos. *Plant Danin* 3:429–436

Somerville GJ, M Sønderskov, SK Mathiassen, H Metcalfe (2020). Spatial modelling of within-field weed populations: A review. *Agronomy* 10:1044

Vasu D, SK Singh, N Sahu, P Tiwary, P Chandran, VP Duraisami, V Ramamurthy, M Lalitha, B Kalaiselvi (2017). Assessment of spatial variability of soil properties using geospatial techniques for farm level nutrient management. *Soil Till Res* 169:25–34

Warrick, A.W., Nielsen, D.R., 1980. Spatial variability of soil physical properties in the field. In: Applications of Soil Physics, pp:319–344. Hillel, D. (Ed.). Academic Press, New York, USA

Yousaf A, N Khalid, M Aqeel, ZF Rizvi, HAS Alhaithloul, W Sarfraz, KA Mutairi, TS Albishi, S Alamri, M Hashem, A Noman, SH Qari (2022). Assessment of composition and spatial dynamics of weed communities in agroecosystem under varying edaphic factors. *PLoS One* 17:e0266778

Zargar M, G Bodner, A Tumanyan, N Tyutyuma, V Plushikov, E Pakina, N Shcherbakova, M Bayat (2018). Productivity of various barley (*Hordeum vulgare* L.) cultivars under semi-arid conditions in southern Russia. *Agron Res* 16:2242–2253